Shape Memory Polymers: Thermomechanical Constitutive Numerical Model

Olaniyi A. Balogun
School of Mechanical and Materials Engineering,
Washington State University Tri-Cities
Richland, WA, USA
olaniyi.balogun@wsue.edu

Changki Mo
School of Mechanical and Materials Engineering,
Washington State University Tri-Cities
Richland, WA, USA
changki.mo@tricity.wsu.edu

Abstract *- In order to predict the thermomechanical behavior of Shape Memory Polymers (SMPs), a one-dimensional rheological thermomechanical constitutive model was adopted and a numerical simulation of this model was developed using a finite element software ABAQUS. The one-dimensional model was selected due to its undemanding material constant requirements which are practical for engineering industrial applications. The model was expanded to a three-dimensional isotropic model and then simulated by means of a user-defined subroutine. The methods of three-dimensional expansion and numerical implementation are presented in this work. Evolution of the internal loads was conducted by making use of the backward difference scheme, which was applied to all quantities within the model, including the material properties. A comparison of the numerical simulation results was carried out with the available experimental data. The Model shows good correlation with experimental results with the capability to predict behaviors such as shape fixity and relaxation.*

Keywords: Shape memory polymers, Constitutive modeling, Thermomechanical analysis, Finite element method, Three-dimensional analysis.

1 Introduction

Shape memory polymers (SMPs) are classified as smart materials. Smart material can sense their environment or their current state, make judgment, and then change their function according to a predetermined purpose [1]. In the case of SMPs, they can be deformed and thereby fixed into a temporary stable shape until it is exposed to an appropriate external stimulus that will trigger the polymer to recover its original shape [2]. SMPs have been around since the 1940's [3] but only in the last two decades has there been detailed research work on their engineering applications and analytical modeling.

Detailed applications of SMPs are noted in many engineering fields. For example, Leindlein et. al. [4] developed a self-tightening suture application for minimum invasive surgery. In 2004, Everhart et. al. [5] developed high temperature reusable SMP mandrels. Thermally-activated SMPs have been applied recently to aircraft skin as shown by McKnight and Henry [6]; Rauscher [7] and to smart joint in a morphing wing (see Manzo and Garcia [8]; Lan *et al.* [9]; Boyerinas *et al.* [10]; Clark *et al.* [11]).

SMPs responding to temperature change will typically undergo a thermo-mechanical behavior under load. Their shape change or deformation tends to be large and nonlinear which invariably needs a detail understanding of the load, stresses and strain before extensive application to aerospace structures. In order to understand the thermomechanical behavior of SMP, comprehensive analytical modeling and experimental validation of the model has been carried out. However, analytical modeling of the behavior for the large deformation of those types of systems is not intuitive. Recent analytical modeling work applying volume fractions approach has been done (see Baghani et al [12]; Lui et al [13]). This paper focuses on developing a simple numerical model that is practical for industrial engineering application with material properties and constants that are easy to derive or measure.

2 Constitutive Model

In order to develop complicated structures using a thermally activated SMPs, it is imperative to understand the fundamental thermomechanical behavior of the material and be able to model this behavior correctly. A numerical constitutive model is presented in this paper based on a previous rheological model that is well known.

2.1 One dimensional model

One factor that will contribute to the commercial aerospace industry adopting SMPs into their structures is the simplification of the constitutive relation and required material properties. Typically, engineers tend to apply allowables and margins over their structures to account for any inaccuracies within constitutive relation all through the build and use of the structure. The selection of the constitutive model was based primarily on engineering application experience at the early stage of this research work.

In 1997, Tobushi *et al.* [14] proposed a one dimensional linear constitutive model for SMPs of Polyurethane series, and this model was selected in this work as a starting point for numerical simulation. Figure 1 shows the rheological model. The model was derived by modifying the standard linear viscoelastic (SLV) model by introducing a slip element due to internal friction and described as a creep irrecoverable strain ε_s.

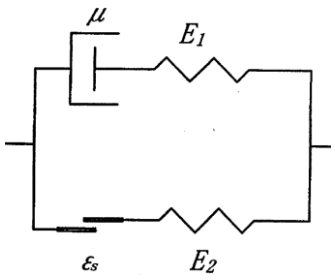

Figure 1. Tobushi's four element rheological model [14]

The constitutive model developed by Tobushi et. al. is given as

$$\dot{\varepsilon} = \frac{\dot{\sigma}}{E} + \frac{\sigma}{\mu} - \frac{\varepsilon - \varepsilon_s}{\lambda} + \alpha \dot{T} \qquad \textbf{(1)}$$

$$\varepsilon_s = C(\varepsilon_c - \varepsilon_l) \qquad \textbf{(2)}$$

$$E = E_g \exp\left[a_E \left(\frac{T_g}{T} - 1 \right) \right] \qquad \textbf{(3)}$$

where σ, ε, μ, λ and α represents stress, strain, viscosity, retardation time and the coefficient of thermal expansion respectively. Also E, T, and C are Young's modulus, temperature and proportionality coefficients. The quantities ε_c, ε_l and T_g represents the creep strain, critical creep strain and glass temperature of the material. C and ε_l shown in equation (2) are temperature dependent. SMPs material properties are highly temperature dependent especially at the glass temperature region [14]. Equation (3) shows how material properties relate with temperature where a_E is derived empirical along with other material properties exponential constants.

2.2 Three dimensional model

The one dimensional model developed by Tobushi et. al. is very similar to Maxwell-Zener model with the exception of slip element introduced. For the purpose of this work, it is assumed that SMPs are isotropic, thus applying the three dimensional Maxwell-Zener model proposed by Ritcher [15] is appropriate. SMPs are polymers regardless of their stiffness change, they still maintain an isotropic property similar to other polymers. The Maxwell-Zener model is composed of a spring arranged in parallel with a maxell viscoelastic element as shown in Figure 2.

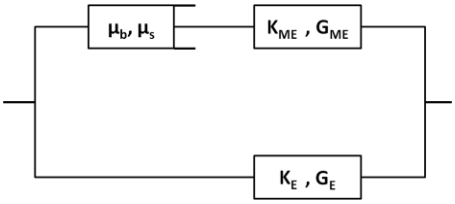

Figure 2. Ritcher's Maxwell-Zener rheological model [15]

The three dimensional model is given as

$$\begin{aligned}
&\left(1 + \frac{G_E}{G_{ME}}\right)\dot{\varepsilon}_{ij} + \frac{1}{3}\left(\frac{K_E}{K_{ME}} - \frac{G_E}{G_{ME}}\right)\delta_{ij} tr(\dot{\underline{\underline{\varepsilon}}}) \\
&+ \frac{G_E}{\mu_s}\varepsilon_{ij} + \frac{1}{3}\left(\frac{K_E}{\mu_b} - \frac{G_E}{\mu_s}\right)\delta_{ij} tr(\underline{\underline{\varepsilon}}) = \\
&\frac{1}{2G_{ME}}\dot{\sigma}_{ij} + \frac{1}{3}\left(\frac{1}{3K_{ME}} - \frac{1}{2G_{ME}}\right)\delta_{ij} tr(\dot{\underline{\underline{\sigma}}}) \\
&+ \frac{1}{2\mu_s}\sigma_{ij} + \frac{1}{3}\left(\frac{1}{3\mu_b} - \frac{1}{2\mu_s}\right)\delta_{ij} tr(\underline{\underline{\sigma}})
\end{aligned} \qquad \textbf{(4)}$$

where the indices i and j are the tensor component of the mechanical strain ($\underline{\underline{\varepsilon}}$) and stress ($\underline{\underline{\sigma}}$) tensors under consideration. The dot represents the derivative with respect to time, the operator *tr()* is the trace of the tensor and δ_{ij} is the Kronecker delta funcion. The derivation of the constitutive equation above as been based on separating the stress tensor into a hydrostatic and deviatoric components. The subscripts *ME*, *E*, *b* and *s* represents the Maxwell, elastic, bulk and shear quantities, respectively while K and G represents the shear and bulk modulus.

2.3 Modified Three dimensional Model

Observing the similarities for both Tobushi and Ritchers model, a modified three dimensional model was developed. The rheological model shown in Figure 3 combines the slip elements from Tobushi's model to the three dimensional model proposed by Ritcher.

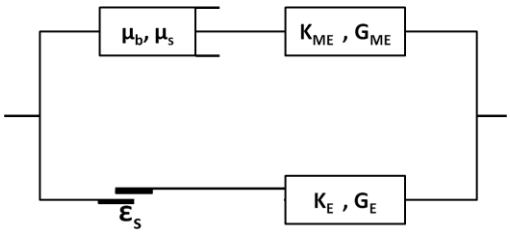

Figure 3. Modified Maxwell-Zener Model incorporating Tobushi's slip element.

Equation 4 can then be modified including the slip element and the thermal interaction within the SMP to give

$$\left(1+\frac{G_E}{G_{ME}}\right)\dot{\varepsilon}_{ij}+\frac{1}{3}\left(\frac{K_E}{K_{ME}}-\frac{G_E}{G_{ME}}\right)\delta_{ij}tr(\dot{\underline{\varepsilon}}) + \frac{G_E}{\mu_s}\left(\varepsilon-\varepsilon_s\right)_{ij}-\left(\frac{G_E}{3\mu_s}\right)\delta_{ij}tr(\underline{\varepsilon}-\varepsilon_s) - \alpha\left(1+\frac{K_E}{K_{ME}}\right)\dot{T}\,\delta_{ij}= \frac{1}{2G_{ME}}\dot{\sigma}_{ij}+\frac{1}{3}\left(\frac{1}{3K_{ME}}-\frac{1}{2G_{ME}}\right)\delta_{ij}tr(\dot{\underline{\sigma}}) + \frac{1}{2\mu_s}\sigma_{ij}-\left(\frac{1}{6\mu_s}\right)\delta_{ij}tr(\underline{\sigma}) \quad \textbf{(5)}$$

The retardation time shown in the equation **(1)** is accounted for as follows

$$\frac{E_E}{3\mu_s}=\frac{1}{\lambda} \quad \textbf{(6)}$$

where E_E will represent the Young's elastic modulus of the the elastic element in equation 1. Equation (5) reduces back to the one-dimensional Equation (1) if Poisson's ratio of both elements are set to zero, the transverse components are ignored, and $E_1>>E_2$.

2.4 Time Discrete Form of Model

The time discrete form of the model developed in the previous section is discussed here. The time discrete model is required for numerical simulation if the model. A backward difference scheme has been employed similar to Ritcher's method to account for evolution of the internal loads within the SMP. For clarity, the strain and stress term have been analyzed separately and then combined after all terms have been simplified.

STRAIN TERM

The Strain Term is given by

$$StrainTerm = \left(1+\frac{G_E}{G_{ME}}\right)\dot{\varepsilon}_{ij}+\frac{1}{3}\left(\frac{K_E}{K_{ME}}-\frac{G_E}{G_{ME}}\right)\delta_{ij}tr(\dot{\underline{\varepsilon}}) + \frac{G_E}{\mu_s}\left(\varepsilon-\varepsilon_s\right)_{ij}-\left(\frac{G_E}{3\mu_s}\right)\delta_{ij}tr(\underline{\varepsilon}-\varepsilon_s) - \alpha\left(1+\frac{K_E}{K_{ME}}\right)\dot{T}\,\delta_{ij} \quad \textbf{(7)}$$

where the strain defined is the total strain. The coefficients are truncated using Greek symbols as

$$-\left(\frac{G_E}{3\mu_s}\right)\rightarrow\lambda_1;\quad \frac{1}{3}\left(\frac{K_E}{K_{ME}}-\frac{G_E}{G_{ME}}\right)\rightarrow\lambda_2 \quad \frac{G_E}{\mu_s}\rightarrow 2\mu_1;\left(1+\frac{G_E}{G_{ME}}\right)\rightarrow 2\mu_2 \quad \textbf{(8)} \quad -\alpha\left(1+\frac{K_E}{K_{ME}}\right)\rightarrow\theta$$

The concise strain term becomes

$$StrainTerm = \lambda_1\delta_{ij}tr(\underline{\varepsilon}-\varepsilon_s)+2\mu_1\left(\varepsilon-\varepsilon_s\right)_{ij} + \lambda_2\delta_{ij}tr(\dot{\underline{\varepsilon}})+2\mu_2\,\dot{\varepsilon}_{ij}+\theta\dot{T}\,\delta_{ij} \quad \textbf{(9)}$$

As mentioned earlier the evolution is done using a backward difference scheme implicitly. Rate quantities are swapped by a finite change divided by a related delta time, while other quantities are augmented by their respective finite increment including the material properties which can change over time as temperature changes. Thus the evolution quantities becomes

$$
\begin{aligned}
&tr\left(\varepsilon-\varepsilon_s\right)_{ij} \rightarrow tr\left(\varepsilon-\varepsilon_s\right)_{ij}+\Delta tr\left(\varepsilon-\varepsilon_s\right)_{ij}\\
&\left(\varepsilon-\varepsilon_s\right)_{ij} \rightarrow \left(\varepsilon-\varepsilon_s\right)_{ij}+\Delta\left(\varepsilon-\varepsilon_s\right)_{ij}\\
&\dot{\varepsilon}_{ij} \rightarrow \frac{\Delta\varepsilon_{ij}}{\Delta t}; tr(\dot{\varepsilon}) \rightarrow \frac{\Delta tr(\varepsilon)}{\Delta t}; \dot{T} \rightarrow \frac{\Delta T}{\Delta t}\\
&\lambda_{1,2} \rightarrow \lambda_{1,2}+\Delta\lambda_{1,2};\ \mu_{1,2} \rightarrow \mu_{1,2}+\Delta\mu_{1,2}\\
&\theta \rightarrow \theta+\Delta\theta
\end{aligned}
\qquad \textbf{(10)}
$$

Applying Equation (10) to (9) and multiplying both sides by a discrete change in time results in

$$
\begin{aligned}
&StrainTerm\times\Delta t =\\
&(\lambda_1+\Delta\lambda_1)\Delta t\delta_{ij}tr(\underline{\underline{\varepsilon}}-\varepsilon_s-\Delta\varepsilon_s)\\
&+2(\mu_1+\Delta\mu_1)\Delta t\left(\varepsilon-\varepsilon_s-\Delta\varepsilon_s\right)_{ij}\\
&+\left[(\lambda_1+\Delta\lambda_1)\Delta t+(\lambda_2+\Delta\lambda_2)\right]\delta_{ij}\Delta tr(\underline{\underline{\varepsilon}})\\
&+2\left[(\mu_1+\Delta\mu_1)\Delta t+(\mu_2+\Delta\mu_2)\right]\Delta\varepsilon_{ij}\\
&+(\theta+\Delta\theta)\Delta T\delta_{ij}
\end{aligned}
\qquad \textbf{(11)}
$$

With further simplification such as

$$
\begin{aligned}
&\left[(\lambda_1+\Delta\lambda_1)\Delta t+(\lambda_2+\Delta\lambda_2)\right] \rightarrow A\\
&2\left[(\mu_1+\Delta\mu_1)\Delta t+(\mu_2+\Delta\mu_2)\right] \rightarrow B\\
&(\theta+\Delta\theta) \rightarrow C
\end{aligned}
\qquad \textbf{(12)}
$$

Equation 11 reduces to

$$
\begin{aligned}
&StrainTerm\times\Delta t =\\
&(\lambda_1+\Delta\lambda_1)\Delta t\delta_{ij}tr(\underline{\underline{\varepsilon}}-\varepsilon_s-\Delta\varepsilon_s)\\
&+2(\mu_1+\Delta\mu_1)\Delta t\left(\varepsilon-\varepsilon_s-\Delta\varepsilon_s\right)_{ij}\\
&+A\delta_{ij}\Delta tr(\underline{\underline{\varepsilon}})+B\Delta\varepsilon_{ij}+C\Delta T\delta_{ij}
\end{aligned}
\qquad \textbf{(13)}
$$

STRESS TERM

Following similar steps as shown for the strain term the stress term can be derived as

$$
\begin{aligned}
&StressTerm\times\Delta t =\\
&F\Delta\sigma_{ij}+D\Delta tr(\underline{\underline{\sigma}})\\
&+\Delta t\left[(\varphi_1+\Delta\varphi_1)tr(\underline{\underline{\sigma}})\delta_{ij}+2(\psi_1+\Delta\psi_1)\sigma_{ij}\right]
\end{aligned}
\qquad \textbf{(14)}
$$

Where the letter and greek symbols represents

$$
\begin{aligned}
&2\left[(\psi_1+\Delta\psi_1)\Delta t+(\psi_2+\Delta\psi_2)\right] \rightarrow F\\
&(\varphi_1+\Delta\varphi_1)\Delta t+(\varphi_2+\Delta\varphi_2) \rightarrow D\\
&\frac{1}{2\mu_s} \rightarrow 2\psi_1;\quad \frac{1}{2G_{ME}} \rightarrow 2\psi_2\\
&-\frac{1}{6\mu_s} \rightarrow \varphi_1;\quad \frac{1}{3}\left(\frac{1}{3K_{ME}}+\frac{1}{2G_{ME}}\right) \rightarrow \varphi_2
\end{aligned}
\qquad \textbf{(15)}
$$

NORMAL STRESS INCREMENTATION

Calculation of the nominal stress incrementation is shown below. In order to derive the incrementation trace stress only the nominal stresses are activated thus $\delta_{ij} = 1$. Applying the backward difference method shown in equation (10) directly to equation (5) and multiply both sides by 3 yields the incrementation trace stress as

$$
\Delta tr(\underline{\underline{\sigma}}) = \frac{H}{G}\left(\Delta tr(\underline{\underline{\varepsilon}})-3\alpha\Delta T\right)
\qquad \textbf{(16)}
$$

where

$$
\begin{aligned}
&\omega+\Delta\omega \rightarrow H\\
&\zeta+\Delta\zeta \rightarrow G\\
&1+\frac{K_E}{K_{ME}} \rightarrow \omega\\
&\frac{1}{3K_{ME}} \rightarrow \zeta
\end{aligned}
\qquad \textbf{(17)}
$$

Finally, an example of the incremental stress in the x direction can now be calculated by setting equations 11 and 14 equal to each other incorporating equation 16 becomes

$$\Delta\sigma_{xx} =$$
$$\frac{\Delta t}{F}(\varepsilon_{xx} - \varepsilon_{sx} - \Delta\varepsilon_{sx})[(\lambda_1 + \Delta\lambda_1) + 2(\mu_1 + \Delta\mu_1)]$$
$$+\frac{\Delta t}{F}((\varepsilon_{yy} - \varepsilon_{sy} - \Delta\varepsilon_{sy}) + (\varepsilon_{yy} - \varepsilon_{sz} - \Delta\varepsilon_{sz}))$$
$$(\lambda_1 + \Delta\lambda_1) + \Delta\varepsilon_{xx}\frac{A + B - \frac{DH}{G}}{F}$$
$$+(\Delta\varepsilon_{yy} + \Delta\varepsilon_{zz})\frac{A - \frac{DH}{G}}{F} \quad \textbf{(18)}$$
$$-\sigma_{xx}\frac{\Delta t}{F}[(\varphi_1 + \Delta\varphi_1) + 2(\psi_1 + \Delta\psi_1)]$$
$$-(\sigma_{yy} + \sigma_{zz})\frac{\Delta t}{F}(\varphi_1 + \Delta\varphi_1)$$
$$+\frac{\Delta T}{F}\left(C + \frac{3\alpha DH}{G}\right)$$

Similar results can be derived for the other normal components of the increment stress tensor.

SHEAR STRESS INCREMENTATION

For shear case the *i* and *j* indices are not equal thus $\delta_{ij} = 0$ thereby simplify the strain and stress term. The shear stress incrementation is resolved below as

$$\Delta\sigma_{ij} =$$
$$\frac{B\Delta\varepsilon_{ij} + 2\Delta t[(\mu_1 + \Delta\mu_1)(\varepsilon - \varepsilon_s - \Delta\varepsilon_s)_{ij} - (\psi_1 + \Delta\psi_1)\sigma_{ij}]}{F} \quad \textbf{(19)}$$

3 Model Validation

The commercial available Finite Element Model (FEM) tool ABAQUS was used to develop the subroutine for this model. Model verification was done by modeling a single quadratic element. The steps applied to the FEM where similar to the steps described in Tobushi's work [14]. A quasi-static steady state step was assumed for all steps within the model. The steps within the FEM includes

1) Applied a pressure of -7e5 Pa to the element at 348K
2) Hold strain constant while elements cools down to 328K
3) Release the strain constrain at 308K
4) Heat element back up to 348K

Results of the FE model were compared to experimental data provided in Tobushi's work [14]. **Error! Reference source not found.** shows stress versus strain curve validation results of the 3D isotropic model for a single element within ABAQUS [16] compared to Tobushi's experimental results. As expected, the stress versus strain curve follows a linear trend for step 1. As temperature cools down in step 2, residual stresses are being stored in the SMPs due to the thermal and mechanical energy interacti.

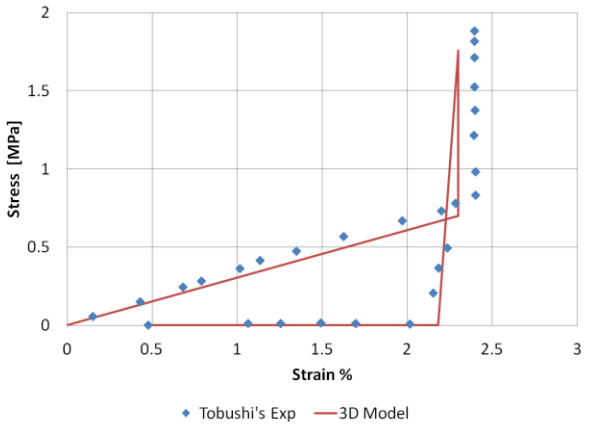

Figure 4. Stress vs. Strain model validation

Figure 5 shows the stress versus temperature curve, The residual stresses stored within the SMP is clearly seen as temperature reduces from 348K to 308K. The model predicts a 1.7MPa residual stress compared to the experimental data which is 1.9MPa.

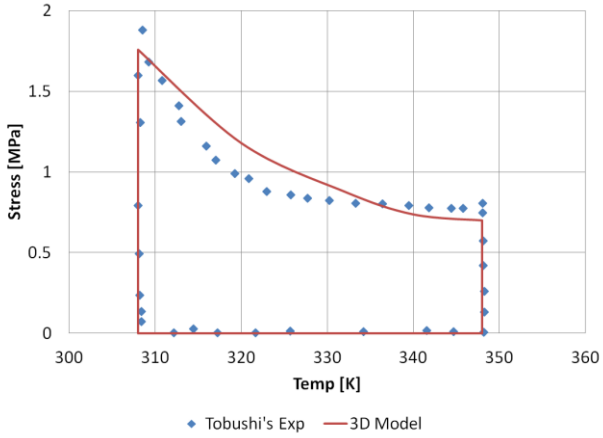

Figure 5. Stress vs. Temperature model validation

Figure 6 shows the strain versus temperature curve. The mechanical strain is kept constant in step 2 as shown in the figure. The current model does not accurately predict

the strain relaxation trend in step 4 due to the simplified SLVS model used. Overall, the model follows the experimental data trends and can be used to model engineering structures with adequate error margin applied.

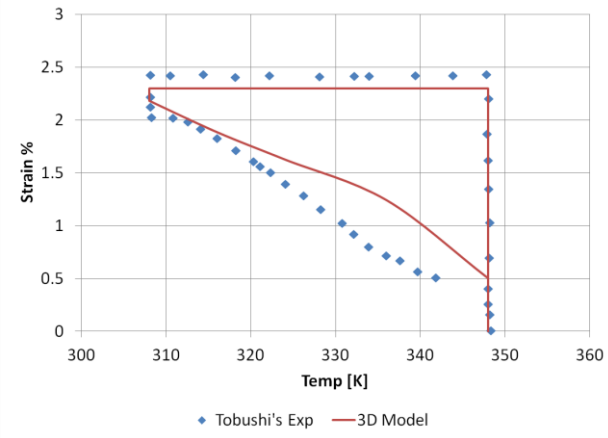

Figure 6. Strain vs. Temperature model validation

4 Conclusion

In this work, a SMP one-dimensional rheological model was selected based on requirement for commercial aerospace application. This model was expanded into a three-dimensional isotropic model. The three-dimensional model was evaluated in a time discrete form so as to apply it in a numerical simulation. Numerical results were compared to already available experimental results for the one-dimensional model. Model shows good correlation with experimental results with the capabitility to predict behaviours such as shape fixity and relaxation

Acknowledgment

The authors acknowledge the Boeing Learning Together Program and WSU New Faculty Seed Grant Program for supporting a part of this work.

References

[1] Z.L. Wang and Z.C. Kang *Functional and smart materials* Plenum Publishing Corp; New York pp 514, 1998.

[2] T. Xie, "Recent advances in Shape Memory Polymer," *Polymer*, Vol. 52, pp.4985 – 5000, 2011.

[3] C. Liu, H. Qin and P. Mather, "Review of Progress in Shape-Memory Polymers," *J Mater Chem*, Vol. 17, pp. 1543-1558, 2007

[4] A. Lendlein, R. Langer, "Biodegradable, Elastic Shape Memory Polymer for Potential Biomedical Application," *Science*, Vol. 296, pp. 1673-1676, May 2002

[5] M.C. Everhart, D.M. Nickerson and R.D Hreha, "High-Temperature Reusable Shape Memory Polymer Mandrels," *Proc. of SPIE, Smart Structures and Materials 2006: Industrial and Commercial Applications of Smart Structures Technologies*, Vol. 6171, 61710K, 2006.

[6] G. McKnight, and C. Henry, "Variable stiffness materials for reconfigurable surface applications," *Proc. of SPIE, Smart Structures and Materials, Active Materials: Behavior and Mechanics*, 5761, pp. 119-129, 2005.

[7] S.G. Rauscher, *Testing and analysis of shape-memory polymers for morphing aircraft skin*, MS Thesis, Mechanical Engineering and Materials Science Department, University of Pittsburgh, 2008.

[8] J.E. Manzo and G. Ephrahim, "The smart joint: model and optimization of a shape memory alloy/shape memory polymer composite actuator," *Proc. of the ASME Conf. on Smart Materials, Adaptive Structures and Intelligent Systems*, 1, pp. 577-583, 2008.

[9] X. Lan, X. Wang, H. Lu, Y. Liu and J. Leng, "Shape recovery performances of a deployable hinge fabricated by fiber-reinforced shape-memory polymer," *Proc. of SPIE, Behavior and Mechanics of Multifunctional Materials and Composites*, 7289, 2009.

[10] B. Boyerinas, *Design and Fabrication of a Variable Stiffness Link for Use in a Morphing Unmanned Air Vehicle*, MS Thesis, Mechanical Engineering and Materials Science Department, University of Pittsburgh, 2009.

[11] W.W. Clark, J.C. Brigham, C. Mo, and S. Joshi, "Modeling of High-Deformation Shape Memory Polymer Locking Link," *Proc. of SPIE, Smart Structures and Materials*, San Diego, CA, 2010.

[12] M. Baghani, R. Naghdabadi, J. Arghavani and S. Sohrabpour, "A thermodynamically-consistent 3D constituitive model for shape memory polymers," *International Journal of Plasticity*, Vol. 30, pp. 13-30, 2012

[13] Y. Liu, K. Gall, M. Dunn, A. Greenberg and J. Diani, "Thermomechanics of shape memory polymers: uniaxial experiments and constitutive modeling," *International Journal of Plasticity*, Vol. 22, pp. 279–313, 2006.

[14] H. Tobushi, T. Hashimoto, S. Hayashi and E. Yamada "Thermomechanical Constitutive Modeling in Shape Memory Polymer of Polyurethane Series," *J. Intel. Mat. Syst. Str.*, Vol 8, pp.711-718, 1997.

[15] F. Ritcher, , *Upsetting and Viscoelasticity of Votreous SiO2: Experiments, Interpretation and Simulation*, PhD

Thesis, Von der Fakultät III – Prozesswissenschaften der Technischen Universität, Berlin, 2006.

[16] Abaqus/Standard, 2011, SIMULIA, Providence RI.